

# Journal of Materials Chemistry B

Accepted Manuscript



This is an *Accepted Manuscript*, which has been through the Royal Society of Chemistry peer review process and has been accepted for publication.

*Accepted Manuscripts* are published online shortly after acceptance, before technical editing, formatting and proof reading. Using this free service, authors can make their results available to the community, in citable form, before we publish the edited article. We will replace this *Accepted Manuscript* with the edited and formatted *Advance Article* as soon as it is available.

You can find more information about *Accepted Manuscripts* in the [Information for Authors](#).

Please note that technical editing may introduce minor changes to the text and/or graphics, which may alter content. The journal's standard [Terms & Conditions](#) and the [Ethical guidelines](#) still apply. In no event shall the Royal Society of Chemistry be held responsible for any errors or omissions in this *Accepted Manuscript* or any consequences arising from the use of any information it contains.

Cite this: DOI: 10.1039/c0xx00000x

www.rsc.org/xxxxxx

ARTICLE TYPE

## A facile microemulsion template route for producing hollow silica nanospheres as imaging agents and drug nanocarriers

Nirun Jatupaiboon<sup>ab</sup>, Yanfang Wang<sup>ab</sup>, Hao Wu<sup>ab</sup>, Xiaojie Song<sup>ab</sup>, Yiche Song<sup>ab</sup>, Jianbin Zhang<sup>ab</sup>, Xiaojun Ma<sup>a\*</sup> and Mingqian Tan<sup>a\*</sup>

Received (in XXX, XXX) Xth XXXXXXXXXX 20XX, Accepted Xth XXXXXXXXXX 20XX

DOI: 10.1039/b000000x

Hollow silica nanospheres with uniform size distribution, tuneable shell thickness were synthesized through a one-step reverse microemulsion method at room temperature within 24 h. These hollow nanospheres demonstrated effective encapsulation ability for FITC, Eu<sup>3+</sup>-complex, iron oxide nanoparticles and chemotherapy drug for potential imaging and drug delivery applications.

Hollow silica nanospheres (HSNs) have recently attracted significant attention owing to their unique property and structure.<sup>1,2</sup> They have been expected to have superior properties compared to solid particle properties, for example, low bulk density, high specific surface area, low thermal conductivity, good encapsulation capacity and unique optical characteristics, because of their inner void encircled by particular solid shell.<sup>3</sup> The nanospheres can encapsulate many agents, such as magnetic or catalytic components,<sup>4</sup> drug/gene,<sup>5, 6</sup> medical diagnostics,<sup>7</sup> inside the hollow cavity. With the progression of nanotechnology, controllable preparation of HSNs has been becoming attractive technique for innovation of further functionalized nanomaterials.

There are many synthetic strategies available for preparation of HSNs, such as the Kirkendall effect,<sup>8</sup> the soft/hard-templating methods,<sup>3, 9-11</sup> galvanic replacement,<sup>12, 13</sup> hydrothermal method,<sup>14</sup> and surface-protected etching.<sup>15,16</sup> Most HSNs were fabricated by soft/hard-templating methods, which need complicated steps to remove the templates after the reaction. For instance, to create inner void space, high temperature calcination or solvent extraction with strong acidic or alkali wash of the core template was inevitable.<sup>16</sup> Such template-assistant methods are effective to produce HSNs with relatively narrow size distribution, but removing the core template may lead to agglomeration, or stick to each other to form larger particles.<sup>17</sup> Moreover, these techniques are often tedious and hard to prepare spheres with size less than hundred nanometers. This limits their effective applications as nanocarriers in biological field due to the poor cell uptake and easy accumulation characteristics within body for *in vivo* drug delivery.<sup>18</sup>

Recently, hollow silica spheres with size around 550 nm were synthesized using spontaneous self-transformation approach in a Stöber solution.<sup>19</sup> The results inspired us to think how to use a self-assembling core as a template to prepare HSNs by designing a facile approach. We have prepared various solid silica nanospheres (SSNs) by using the water-in-oil (W/O) reverse

microemulsion strategy for effective time-resolved fluorescence immunoassay.<sup>20-25</sup> W/O microemulsion offers the advantages in giving uniform sub-100 nm silica nanospheres because the small W/O droplets are thermodynamically stable in the size less than hundred nanometers. Although, a sol-gel method using W/O microemulsion as the template has been applied to prepare HSNs.<sup>17</sup> It required the addition of aminopropyltrimethoxysilane (APS) ethanolic solution and water to soak the product over 7 days to form the hollow spheres, which is too time-consuming. The resulting products are the mixture of small hollow nanospheres (~ 40 nm) and larger yolk-shell nanospheres (~160 nm). As a result, these HSNs are limited in the applications, particularly, in biomedical fields. Therefore, the controllable synthesis of HSNs with the size less than 50 nanometers by a facile approach is still a great challenge.

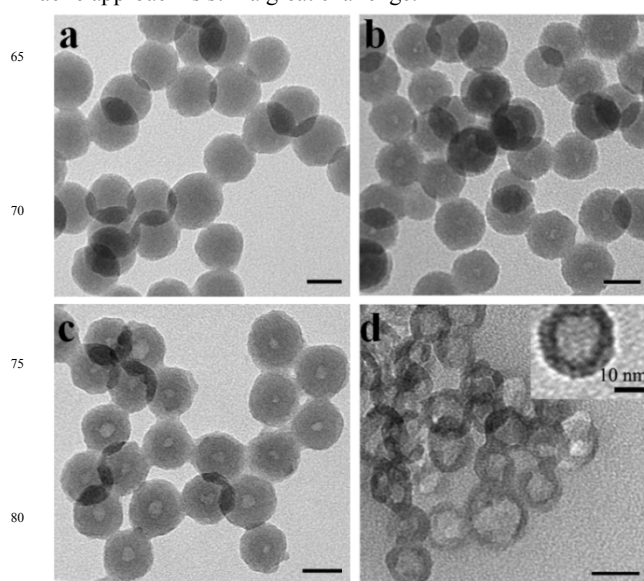


Fig. 1 TEM images of hollow silica nanospheres (HSNs) prepared with (a) 0 L, (b) 1 L, (c) 2 L and (d) 3 L of APS. Scale bar: 25 nm. The inset shows high-magnification TEM image of the HSNs prepared with 3 L of APS.

With the aim of using the advantages of W/O microemulsion as template, we report here for the first time of the preparation of HSNs (<50 nm) and their applications in doping fluorescent dyes, magnetic nanoparticles and anticancer drug for potential imaging and therapy purpose. The HSNs were synthesized by one-step

method using a modified W/O reverse microemulsion system containing APS, Triton X-100, *n*-hexanol, cyclohexane and water, a well-studied system for synthesis of silica nanoparticles with the size less than hundred nanometers.<sup>22</sup> In a typical synthesis, the appropriate amount of APS was added to 1.1 mL of deionized water, followed by adding the mixture into organic phase containing 14.5 g of cyclohexane, 4.47 g of Triton X-100 and 3.64 g of *n*-octanol. After adding 200  $\mu$ L of tetraethyl orthosilicate (TEOS), the polymerization was triggered with 200  $\mu$ L of  $\text{NH}_4\text{OH}$  and continued for 24 h (Scheme S1). The HSNs were obtained after washing with ethanol and water. Fig.1 shows the transmission electron microscopy (TEM) images of HSNs. Without adding the APS, the final product was SSNs (Scheme S2, Fig.1a). If the APS was added (Fig.1b, c, d), a noticeable contrast between the core and the shell was observed, which confirmed the formation of the hollow structure. The exact sizes and core sizes of different hollow nanospheres are listed in Table S1 (ESI<sup>†</sup>). In particular, we demonstrated that the thickness of the shell, the diameter of the cavity can be well adjusted by precise tuning of the reaction parameters. As the amount of APS was increased, the proportion of the core/shell size increased, which was consistent with the result of previous report.<sup>17</sup> The HSNs underwent a spontaneous morphology change from solid to hollow when they were washed with ethanol and water by such a simple etching-free strategy.

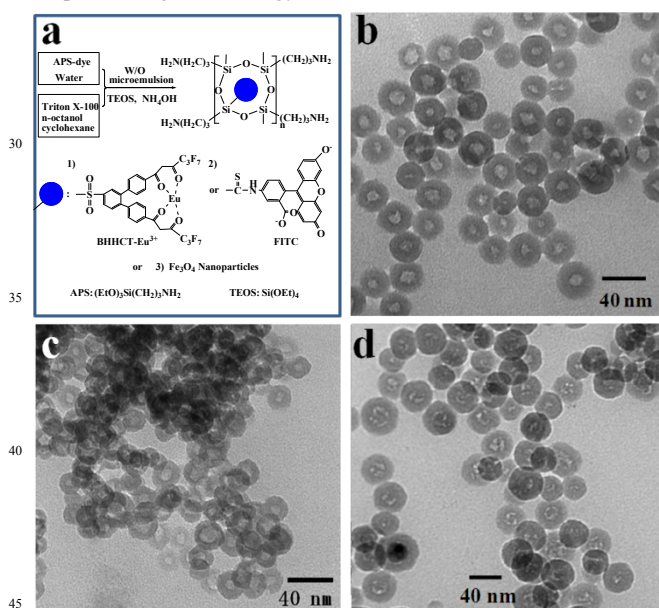
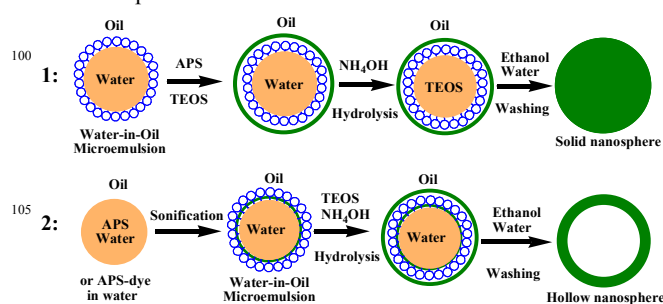


Fig. 2 (a) Schematic illustration for the synthesis of dye-doping HSNs. TEM images of (b) Eu-HSNs, (c) FITC-HSNs (d)  $\text{Fe}_2\text{O}_3$ -HSNs.

The thus-designed HSNs allow the proper loading with guest dye molecules, such as long life-time fluorescence BHHCT- $\text{Eu}^{3+}$  complex, fluorescein isothiocyanate (FITC) and  $\text{Fe}_2\text{O}_3$  magnetic nanoparticles, to fabricate functional nanospheres. Fig. 2a shows the synthesis process of the functional HSNs. Detailed procedure can be found in Scheme S3, S4, S5 of ESI<sup>†</sup>. For example, the BHHCT- $\text{Eu}^{3+}$  doped HSNs (Eu-HSNs) have an average diameter of 32 nm and a mean shell thickness of about 8 nm. The HSNs are significantly monodispersed, smooth and uniform. The size distribution is quite narrow (26 ~36 nm) (Fig. 2b). The average size of FITC-doped HSNs (FITC-HSNs) was about 23 nm with a

10 nm core (Fig. 2c). Interestingly, the TEM image of the  $\text{Fe}_2\text{O}_3$  nanoparticles doped HSNs ( $\text{Fe}_2\text{O}_3$ -HSNs) shows a clear contrast of the iron nanoparticles among the inside core (Fig. 2 d). The shell thickness is estimated to be about 11 nm. We also prepared HSNs doped with both BHHCT- $\text{Eu}^{3+}$  and  $\text{Fe}_2\text{O}_3$  nanoparticles ( $\text{Eu}@\text{Fe}_3\text{O}_4$ -HSNs) (Scheme S6), which possessed both fluorescence emission and magnetic resonance imaging ability (Table S1 and Fig. S1). The good capsulation capacity of the prepared HSNs might be useful as nanocarriers for various biomedical applications. Furthermore, the hollow mesoporous silica nanospheres (HMSNs) were prepared by adding the pore-generating reagent (cetyltrimethylammonium bromide, CTAB) in the reaction. CTAB templates were removed by acidic ethanol extraction, resulting in uniform HMSNs (Fig. S2, Table S1) possessing a 36 nm diameter and a 12 nm core.

Nitrogen absorption and desorption results of the HSNs and Eu-HSNs showed that the hysteresis loops located in the  $p/p_0$  range of 0.8-1.0 (Fig. S3) associated with the presence of large mesopores arising from intraparticle mesoporosity, which were attributed to the void inside of the hollow nanospheres.<sup>26, 27</sup> The Brunauer-Emmett-Teller (BET) surface area and pore volume are calculated to be  $70 \text{ m}^2\cdot\text{g}^{-1}$  and  $0.31 \text{ m}^3\cdot\text{g}^{-1}$  for HSNs,  $83 \text{ m}^2\cdot\text{g}^{-1}$  and  $0.30 \text{ m}^3\cdot\text{g}^{-1}$  for Eu-HSN, respectively. The pore size distribution measured from Barrett-Joyner-Halenda (BJH) method showed a peak at 17 nm for HSNs and 16 nm for Eu-HSNs (Fig. S4), which agreed well with the hollow interior diameter observed from TEM image (Fig.1 d and HSNs3 in Table S1; Fig. 2b and Eu-HSNs in Table S1, ESI<sup>†</sup>). In comparison, the nitrogen absorption and desorption isotherms of HMSNs showed all were of type VI curve with a large hysteresis loop in the  $p/p_0$  range of 0.15-0.95 (Fig. S5), revealing the microporous and mesoporous nature of the materials with narrow size distribution. The surface area and pore volume increased to  $235 \text{ m}^2\cdot\text{g}^{-1}$  and  $0.46 \text{ m}^3\cdot\text{g}^{-1}$  for HMSNs,  $209 \text{ m}^2\cdot\text{g}^{-1}$  and  $0.43 \text{ m}^3\cdot\text{g}^{-1}$  for mesoporous Eu-HSNs, respectively. The step-like shape of the curve near  $p/p_0 \sim 0.15$  clearly indicated some microporous exist on the shell.<sup>17</sup> The pore size of HMSNs was calculated to be about 3.33 nm (Fig. S6). Thus, the HMSNs prepared by such facile microemulsion template route with larger surface area and pore volume would be much better for loading more components.



Scheme 1. Proposed mechanism of the formation of HSNs.

The proposed formation mechanism of the HSNs is shown in Scheme 1. In traditional synthesis of method 1, if APS and TEOS were added to the reverse W/O microemulsion by the copolymerization initiated with ammonia, only SSNs were obtained despite the thorough washing of the final product. In contrast, in method 2, the initial hydrolysis of APS was triggered by reacting with water before adding to the organic phase to form



W/O microemulsion and the oligomer might be produced at interface between W/O. After the polymerization of TEOS triggered by ammonia, the small oligomer would be washed out with ethanol and water to produce the HSNs. The deduction was confirmed by the results shown in Fig. S 7. The nanospheres prepared by method 1 were solid (Fig. S7-a) despite repeated washing with the ethanol and water. However, those prepared with method 2 were SSNs before washing (Fig. S7-b) and HSNs (Fig. S7-c) after thorough washing with ethanol and water. All the processes could be completed within 24 h. The repeated washing step under ultrasonication was necessary for the removal of the small core parts, resulting in the formation of HSNs. Compared with the available methods for preparing HSNs, our strategy has three advantages. First, the shell thickness, core size and cavity volume of HSNs prepared using this method are tuneable. Second, the synthesis process of the HSNs can be completed at room temperature within 24 h, which is much shorter than the reported method (7 days).<sup>17</sup> No heating at 35 °C<sup>19</sup> or template-etching steps are required,<sup>18</sup> which allows eco-friendly synthesis of HSNs at low cost. Third, the W/O microemulsion strategy enables encapsulation of cargo inside the final HSNs and this strategy can be generally used for fabrication of multifunctional nano-devices.

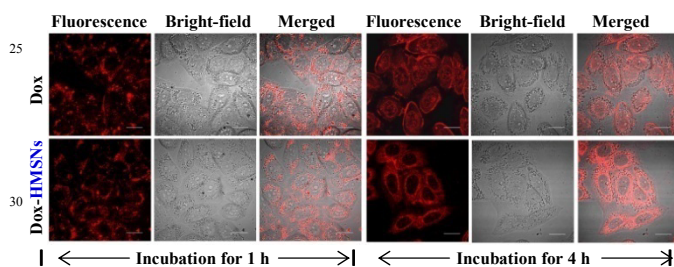


Fig. 3. Confocal laser scanning microscopy images of HeLa Cells incubated with free Dox and Dox-HMSNs at the Dox concentration of 10.0 µg/mL.

To evaluate the potential applications of the FITC-HSNs as imaging agents, they were successfully internalized into human SH-SY5Y neuroblastoma cells (Fig. S8). The fluorescence signal can be seen as long as 6 days. To use HMSNs as drug delivery vehicles, doxorubicin (Dox) was loaded into the HMSNs. The drug entrapment efficiency and loading content of Dox-HMSNs were 94 and 32 wt %, respectively. The Dox loading content was higher than previous works due to the increased nanospheres cavity.<sup>28</sup> An efficient drug delivery system should not only have the capacity to store and delivery drug molecules, but also possess a sustained-release property. Fig. S 9 shows the Dox release profile for Dox-HMSNs at pH 7.4 in PBS buffer at 37 °C. Notably, the release rate of absorbed Dox from the Dox-HMSNs was lowered than those of Dox-HSNs and Dox-SSNs, indicating an obvious sustained release property. This is useful for those clinical cases required a more stable release of smaller dosage. Furthermore, the *in vitro* cell uptake of Dox-HMSNs was verified by confocal laser scanning microscopy (CLSM) after incubation with HeLa cells for 1 and 4 h, respectively. As revealed by Fig. 3, we can see that the Dox-HMSNs and Dox were uniformly distributed in the membrane cytoplasmic area of the tumor cells after 1 h incubation, whereas the Dox-HMSNs remained in the cytoplasm and free Dox entered into the cellular nuclear after 4 h

incubation. This was further supported by the overlay of the bright field and fluorescent imaging. The result indicated that the HMSNs nanocarriers can change the drug distribution and can prevent the decomposition of the drugs prior to reaching the targeted site, enhancing the delivery efficiency.

The cytotoxicity tests of the empty nanocarriers, HMSNs, were conducted against HeLa cells by conducting MTT (3-[4,5-dimethylthiazol-2-yl]-2,5-diphenyltetrazolium bromide) assays. Fig. S10 shows the effect of concentration of HMSNs, Dox-HMSNs and free Dox on the cell viability for different incubation time periods. The Dox-HMSNs exhibited a similar cytotoxicity as free Dox and become greater along with the time increasing from 24 h to 48 h and 72 h. There is no apparent cytotoxicity after incubation at a very high concentration up to 200 µg/mL of HMSNs nanocarriers. The low toxicity of HMSNs guarantees the practical applications as a sustained release drug delivery nanocarrier.

## Conclusions

A facile microemulsion template route for producing hollow silica nanospheres was developed and it could be carried out at room temperature without the use of etching toxic solvent. The prepared HSNs and HMSNs were spherical, uniform and the core size and cavity volume could be tuneable. These HMSNs have high encapsulation capacity and were successfully used as nanocarriers for imaging agents and chemotherapy drug. It is reasonable to believe that the new strategy is promising for preparing HMSNs as delivery vehicles for cancer theranostic applications.

## Author Contributions

Nirun Jatupaiboon and Yanfang Wang contributed equally to this work.

## Acknowledgements

This work was supported by the National Nature Science Foundation of China (91227126), National Special Fund for Key Scientific Instrument and Equipment Development (2013YQ17046307) and the Nature Science Foundation of Liaoning Province, China (2013020177).

## Notes and references

- <sup>a</sup> Division of Biotechnology, Dalian Institute of Chemical Physics, Chinese Academy of Sciences, Dalian 116023, China. Fax & Tel: +86-411-84379139; E-mail: [maxj@dicp.ac.cn](mailto:maxj@dicp.ac.cn), [mqtan@dicp.ac.cn](mailto:mqtan@dicp.ac.cn)  
<sup>b</sup> University of the Chinese Academy of Sciences, Beijing 100049, China

Electronic Supplementary Information (ESI) available: [details of any supplementary information available should be included here]. See DOI: 10.1039/b000000x/

- J. Liu, F. Fan, Z. Feng, L. Zhang, S. Bai, Q. Yang and C. Li, *J Phys Chem C*, 2008, **112**, 16445-16451.
- R. M. Anisur, J. Shin, H. H. Choi, K. M. Yeo, E. J. Kang and I. S. Lee, *J Mater Chem*, 2010, **20**, 10615-10621.
- M. Fuji, T. Shin, H. Watanabe and T. Takei, *Adv Powder Technol*, 2012, **23**, 562-565.
- C. H. Lin, X. Y. Liu, S. H. Wu, K. H. Liu and C. Y. Mou, *J Phys Chem Lett*, 2011, **2**, 2984-2988.
- Y. Chen, H. R. Chen, L. M. Guo, Q. J. He, F. Chen, J. Zhou, J. W. Feng and J. L. Shi, *ACS Nano*, 2010, **4**, 529-539.
- F. Q. Tang, L. L. Li and D. Chen, *Adv Mater*, 2012, **24**, 1504-1534.

7. Y. Chen, H. R. Chen, Y. Sun, Y. Y. Zheng, D. P. Zeng, F. Q. Li, S. J. Zhang, X. Wang, K. Zhang, M. Ma, et al., *Angew Chem Int Edit*, 2011, **50**12505 -12509.
8. K. An and T. Hyeon, *Nano Today*, 2009, **4**, 359-373.
9. F. Caruso, R. A. Caruso and H. Mohwald, *Science*, 1998, **282**, 1111-1114.
10. X. J. Zhou, X. Cheng, W. Feng, K. X. Qiu, L. Chen, W. Nie, Z. Q. Yin, X. M. Mo, H. S. Wang and C. L. He, *Dalton T*, 2014, **43**11834 -11842.
11. R. M. Li, L. Li, Y. H. Han, S. L. Gai, F. He and P. P. Yang, *J Mater Chem B* 2014, **2**, 2127-2135.
12. Y. G. Sun and Y. N. Xia, *J Am Chem Soc*, 2004, **126**, 3892-3901.
13. S. E. Skrabalak, J. Y. Chen, Y. G. Sun, X. M. Lu, L. Au, C. M. Cobley and Y. N. Xia, *Accounts Chem Res*, 2008, **41**1587 -1595.
14. S. K. Das, M. K. Bhunia, D. Chakraborty, A. R. Khuda-Bukhsh and A. Bhaumik, *Chem Commun*, 2012, **48**2891 -2893.
15. Q. Zhang, T. R. Zhang, J. P. Ge and Y. D. Yin, *Nano Lett*, 2008, **8**, 2867-2871.
16. Q. Zhang, I. Lee, J. P. Ge, F. Zaera and Y. D. Yin, *Adv Funct Mater*, 2010, **20**2201 -2214.
17. Y. S. Lin, S. H. Wu, C. T. Tseng, Y. Hung, C. Chang and C. Y. Mou, *Chem Commun*, 2009, 3542-3544.
18. D. Chen, L. L. Li, F. Q. Tang and S. O. Qi, *Adv Mater*, 2009, **21** 3804-3807.
19. Z. G. Teng, X. D. Su, Y. Y. Zheng, J. Sun, G. T. Chen, C. C. Tian, J. D. Wang, H. Li, Y. N. Zhao and G. M. Lu, *Chem Mater*, 2013, **25** 98-105.
20. X. D. Hai, M. Q. Tan, G. Wang, Z. Q. Ye, J. L. Yuan and K. Matsumoto, *Anal Sci*, 2004, **20**245 -246.
21. M. Q. Tan, G. L. Wang, X. D. Hai, Z. Q. Ye and J. L. Yuan, *J Mater Chem*, 2004, **14**2896 -2901.
22. M. Q. Tan, Z. Q. Ye, G. L. Wang and J. L. Yuan, *Chem Mater*, 2004, **16**, 2494-2498.
23. Z. Q. Ye, M. Q. Tan, G. L. Wang and J. L. Yuan, *J Mater Chem*, 2004, **14**851 -856.
24. Z. Q. Ye, M. Q. Tan, G. L. Wang and J. L. Yuan, *Anal Chem*, 2004, **76**, 513-518.
25. Z. Q. Ye, M. Q. Tan, G. L. Wang and J. L. Yuan, *Talanta*, 2005, **65** 206-210.
26. Q. Hu, J. J. Li, S. Z. Qiao, Z. P. Hao, H. Tian, C. Y. Ma and C. He, *J Hazard Mater*, 2009, **164**, 1205-1212.
27. Z. X. Yang, Y. D. Xia and R. Mokaya, *Adv Mater*, 2004, **16**, 727-732.
28. T. Wang, F. Cha, Q. Fu, L. Zhang, H. Liu, L. Li, Y. Liao, Z. Su, C. Wang, B. Duan, et al., *J Mater Chem*, 2011, **21**5299 -5306.

45

Hollow silica nanospheres with uniform size distribution, tuneable shell thickness were synthesized through a one-step reverse microemulsion method at room temperature within 24 h.

